7-1970

Determination of (n, 2n) Reaction Cross-Sections for 71Ga, 106Cd & 138Ba Using 14 MeV Neutrons

Thomas Helm
Western Kentucky University

Helms,

Thomas E.

1970

DETERMINATION OF (n,2n) REACTION CROSS-SECTIONS FOR ^{71}Ga, ^{106}Cd AND ^{138}Ba USING 14 MeV NEUTRONS

BY

THOMAS E. HELMS

A THESIS

SUBMITTED IN PARTIAL FULFILLMENT

OF THE REQUIREMENTS FOR THE DEGREE OF

MASTER OF SCIENCE IN ENGINEERING PHYSICS

WESTERN KENTUCKY UNIVERSITY

JULY 1970

DETERMINATION OF (n,2n) REACTION CROSS-SECTIONS FOR ^{71}Ga, ^{106}Cd AND ^{138}Ba USING 14 MeV NEUTRONS

APPROVED July 28, 1970:
(Date)

W. L. Humphreys
Director of Thesis

W. T. Sisk

C. A. Logan

John Dean Minter
Dean of the Graduate School

ACKNOWLEDGMENTS

The author wishes to express his sincere thanks to Dr. D. L. Humphrey for his direction, encouragement, and work as thesis director. He would like to extend his appreciation to the Faculty Research Fund of Western Kentucky University for its financial assistance.

TABLE OF CONTENTS

LIST OF TABLES

ILLUSTRATIONS

ABSTRACT

Activation cross-sections for the (n,2n) reaction have been measured at an incident neutron energy of 14.7 ± 0.3 MeV for the isotopes ^{71}Ga, ^{106}Cd and ^{138}Ba. These measurements were made relative to the cross-section for the $^{63}Cu(n,2n)^{62}Cu$ reaction. The relative cross-sections were then converted to absolute cross-sections by using the 550 ± 28 mb cross-section value for the $^{63}Cu(n,2n)^{62}Cu$ reaction. Highly enriched isotopes were used as samples.

I. INTRODUCTION

The increasing trend towards the use of activation analysis as an analytic means of identifying elements and determining their relative abundance demands more accurate values of reaction cross-sections. Accurate values of cross-sections are also important in the investigation of possible shell effects in reaction mechanisms. Many activation cross-sections for reactions produced by 14 MeV neutrons have been measured because of the relative ease with which this energy of neutrons can be produced. Low voltage accelerators are capable of producing 14 MeV neutrons by the $^{3}H(d,n)^{4}He$ reaction. Although many people[1-5] have measured the (n,2n) reaction cross-sections for a multitude of stable isotopes, their values differ considerably for a particular range or they report large uncertainties in their measured values. By using improved counting and flux monitoring techniques, an attempt will be made to more accurately determine the values of the (n,2n) reaction cross-sections for ^{71}Ga, ^{106}Cd, and ^{138}Ba.

The values for the (n,2n) reaction cross-sections for these three isotopes are determined by the simultaneous activation of the isotope in question and two copper disks. Each sample is sandwiched between the two foils during activation. Since the $^{63}Cu(n,2n)^{62}Cu$ reaction cross-section

for 14 MeV neutrons has been accurately measured, the activity produced in the copper disks is used in the determination of the (n,2n) reaction cross-sections. The purpose of this thesis is to more accurately determine the values of the (n,2n) reaction cross-sections for ^{71}Ga, ^{106}Cd, and ^{138}Ba by improved techniques.

II. THEORY OF ACTIVATION ANALYSIS

The theory of neutron activation analysis is relatively simple and well known. If a sample containing N nuclei of a particular nuclide having atomic number Z and mass number A is exposed to a source of neutrons of flux $\emptyset$, the rate of formation of a particular nuclide by some reaction is simply:

$$-dN/dt = dN^*/dt = N\emptyset\sigma, \qquad (1)$$

where σ is the isotopic cross-section for a particular reaction induced by neutrons of some fixed energy range and N^* is the number of product nuclei formed.

If the reaction product is a radioactive nuclei with a half-life $T_{\frac{1}{2}}$, its disintegration rate at any time during the irradiation will be:

$$-dN^*/dt = \lambda N^*, \qquad (2)$$

where λ is the disintegration constant. Thus the rate of formation of the radioactive nuclei produced by this particular reaction is:

$$dN^*/dt = N\emptyset\sigma - \lambda N^*. \qquad (3)$$

Upon integration, equation (3) becomes:

$$N^* = N\emptyset\sigma[1 - \exp(-\lambda t_i)]/\lambda. \qquad (4)$$

Since $N^*\lambda$ is the disintegration rate of this radioactive nuclide, equation (4) is usually written as:

$$A_o = N\phi\sigma[1 - \exp(-\lambda t_i)]. \qquad (5)$$

A_o represents the activity of the radioactive nuclide at the completion of activation time t_i.

The inability to begin counting the rate of decay of the radioactive sample produced immediately upon completion of irradiation, necessitates an adjustment to equation (5) to compensate for the loss of activity during the time of transfer of the sample from the irradiation chamber to the counting chamber. The number of disintegrations per second A, of the nuclide at the end of time t_t, between the end of irradiation and the start of counting is related to the absolute activity A_o, by the following expression:

$$A = A_o\exp(-\lambda t_t). \qquad (6)$$

This relationship enables the activity of the sample to be determined upon the completion of the transfer of the sample to the counting chamber. The activation analysis equation (5) now becomes:

$$A = N\phi\sigma[1 - \exp(-\lambda t_i)]\exp(-\lambda t_t). \qquad (7)$$

When the decay of a radioactive sample is followed as a function of time, the counting rate is usually taken to represent the activity at the midpoint of the counting interval Δt. When $\Delta t \ll T_{\frac{1}{2}}$, this approximation is quite good since the rate of decay during Δt is small. This approximation

no longer holds however, when the counting interval is comparable to or greater than the half-life of the sample. As the counting interval increases, the fraction of radioactive nuclei present decreases exponentially. This means that most of the decays occur during the first half of the counting interval. The average activity A, then represents the activity of the sample at some instant of time t_a which occurs earlier than the midpoint of the counting interval Δt. The average activity is then related to the absolute activity and t_a by the following expression:

$$A = A_o \exp(-\lambda t_a). \tag{8}$$

The average activity is also related to the absolute activity and Δt by the following expression:

$$A = \frac{\int_{t_t}^{t_t + \Delta t} A_o e^{-\lambda t} dt}{\Delta t}, \tag{9}$$

where t_t represents the time between the end of irradiation and the start of counting and Δt the counting interval. Integration of this equation yields the following:

$$A = A_o[\exp(-\lambda t_t) - \exp(-\lambda t_t - \lambda \Delta t)]/\lambda \Delta t. \tag{10}$$

Combining equations (8) and (10) yields the following expression:

$$A_o \exp(-\lambda t_a) = A_o[\exp(-\lambda t_t) - \exp(-\lambda t_t - \lambda \Delta t)]/\lambda \Delta t. \tag{11}$$

Equation (11) can be expressed in the form:

$$t_a = t_t + [\ln \lambda \Delta t - \ln(1 - e^{-\lambda \Delta t})]/\lambda. \tag{12}$$

Equation (12) reduces by approximation to:

$$t_a = t_t + f\Delta t, \tag{13}$$

where:

$$f = 1/2 - \lambda\Delta t/24. \tag{14}$$

The graph in Figure 1 shows the relationship between f and $\Delta t/T_{\frac{1}{2}}$ as computed using equation (12). Figure 2 is a representative plot of a hypothetical isotope showing the activity as a function of time. Also indicated in Figure 2 are the relationships among the various time intervals of the activation, transfer and counting of a sample.

For those samples which have short half-lives, the activation equation (7) should be rewritten as follows:

$$A = N\emptyset\sigma[1 - \exp(-\lambda t_i)]\exp(-\lambda t_a). \tag{15}$$

If a detector were capable of detecting all of the radiation emitted by a radioactive sample, equation (15) in its present form would enable one of several parameters such as the flux, the cross-section, or the number of nuclei present to be determined. Since no such detector exists, a further correction must be made in equation (15) to determine the absolute activity of the radioactive nuclide produced.

The number of disintegrations that will be detected by a detector depends upon several factors. Among these are the branching ratio of the particular nuclide, the overall efficiency of the detector, self absorption by the sample, and the peak-to-sum ratio if a gamma scintillation counter is used. These factors are related to the activity by

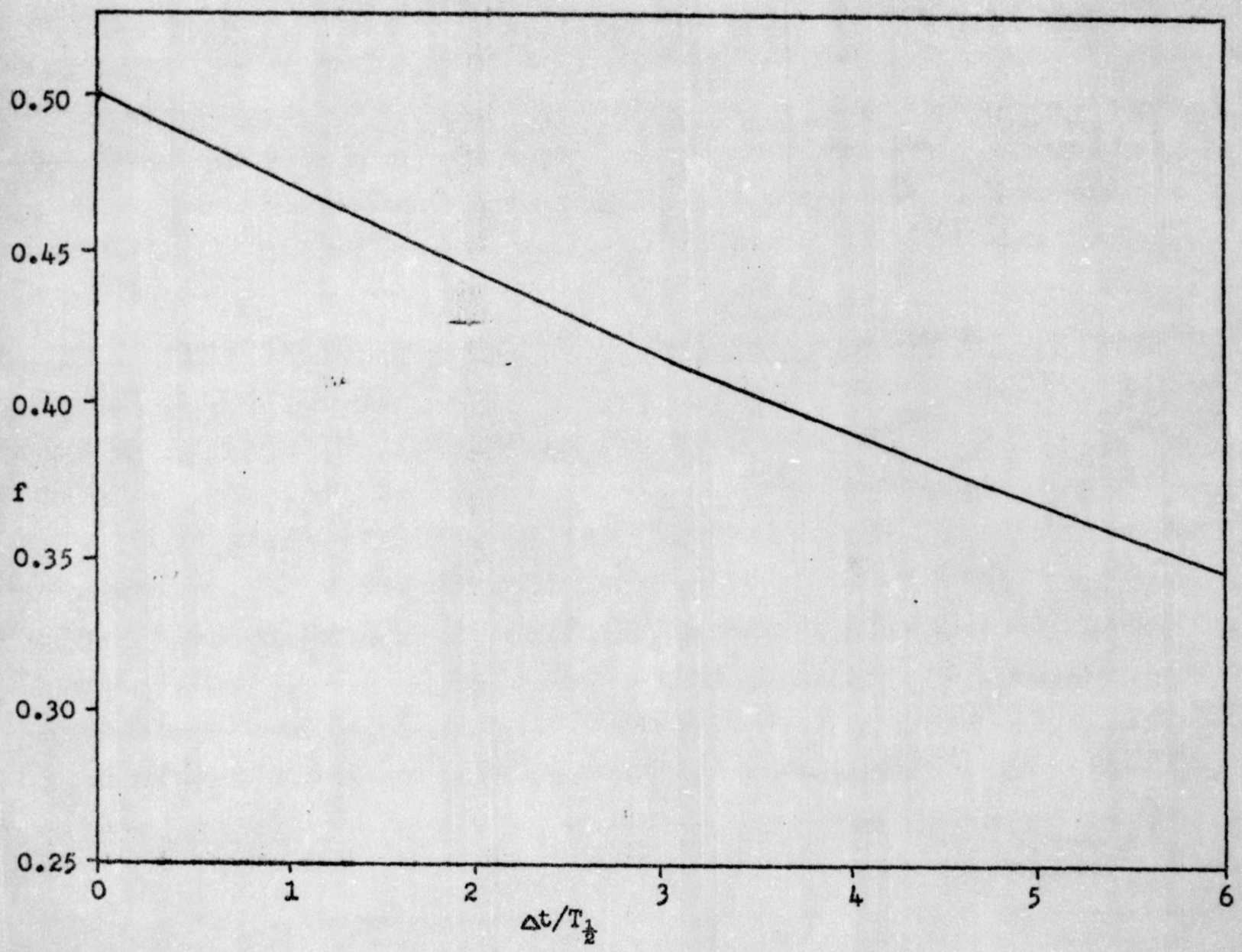

FIGURE 1. THE VARIATION OF f WITH $\Delta t/T_{\frac{1}{2}}$

t_i = irradiation time

t_t = time between the end of irradiation and the start of counting

Δt = counting interval

$f\Delta t$ = correction for loss of activity during counting

t_a = time between end of irradiation and determination of activity

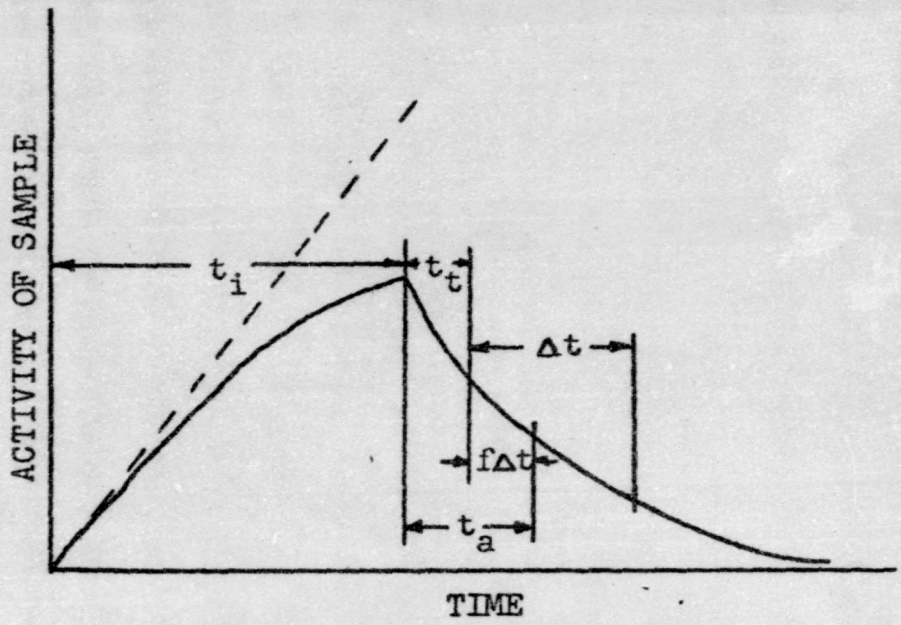

FIGURE 2. SAMPLE ACTIVITY AS A FUNCTION OF TIME

the following expression:

$$A = \frac{A'}{EPRS}, \tag{16}$$

where: A = activity

A' = activity recorded

E = overall detector efficiency

P = peak-to-sum ratio

R = branching ratio

S = self absorption factor.

Combining equations (15) and (16) results in the following expression:

$$A' = EPRSN\emptyset\sigma[1 - \exp(-\lambda t_i)]\exp(-\lambda t_a). \tag{17}$$

The number of nuclei present in the sample can be determined by the equation:

$$N = \frac{W\Theta N_o}{M}, \tag{18}$$

where: W = mass of the element in grams

N_o = Avagadro's number

Θ = isotopic abundance of the nuclide

M = atomic mass of the element.

Since the experiments to be performed are those in which the cross-sections for various reactions produced by neutrons are to be determined, equations (17) and (18) are combined and written in the following form:

$$\sigma = \frac{A'M}{EPRSW\Theta N_o\emptyset[1 - \exp(-\lambda t_i)]\exp(-\lambda t_a)}. \tag{19}$$

While the sample is being activated, the neutron output of the generator is monitored by two methods. A neutron sensitive counter is placed near the generator. The neutron output determined from this counter is not used directly in the activation equation, but is a means of monitoring the stability of the neutron generator. The neutron flux at the sample position is determined by the simultaneous activation of the sample and two copper disks. By placing the sample between the two copper disks, the disks and sample are exposed to the same neutron flux. Using the $^{63}Cu(n,2n)^{62}Cu$ reaction cross-section and the ^{62}Cu activity produced during irradiation, the neutron flux can be determined by solving equation (19) for ϕ. This yields the following expression:

$$\phi = \frac{A'_m M_m}{\sigma_m E_m P_m R_m S_m W_m \Theta_m N_o [1 - \exp(-\lambda_m t_i)] \exp(-\lambda_m t'_a)}, \quad (20)$$

where the subscript m indicates those values pertaining to the monitoring sample.

The copper disks are used as a comparative standard, therefore eliminating the need for accurately controlling and measuring the neutron flux which is highly dependent upon several parameters of the generator. When this comparative type of measurement is done, the activation equation used for determining cross-sections can be expressed as follows:

$$\sigma = \frac{\sigma_m A' M W_m \Theta_m E_m P_m R_m S_m [1 - \exp(-\lambda_m t_i)] \exp(-\lambda_m t'_a)}{A'_m M_m W \Theta E P R S [1 - \exp(-\lambda t_i)] \exp(-\lambda t_a)}. \quad (21)$$

III. EQUIPMENT AND EXPERIMENTAL PROCEDURE

The Neutron Generator

In the activation of the samples to be studied, a Kaman Nuclear Model A-702 neutron generator is used. This generator is shown in Figure 3. This generator utilizes the $^{3}H(d,n)^{4}He$ reaction to generate neutrons with an energy in the 14 MeV range. These neutrons occur in pulsations at a rate of 60 per second to provide an average maximum output of greater than 10^{9} neutrons per second. These pulsations occur at intervals of 16.7 milliseconds and have a half-amplitude width of 5 milliseconds. The maximum neutron flux generated by this accelerator is approximately 10^{8} neutrons per square centimeter per second at the sample activation position.(6)

The neutron generator is a positive ion accelerator with a Penning Ion Gauge type of source.(6) The neutrons are produced by the ionization of deuterium gas in the Penning Ion Gauge. These positive ions are then extracted into the accelerating section where a 144 kv peak potential accelerates them into the target assembly. The focus on this ion beam produces a spot size of $\frac{1}{2}$ inch diameter at the target.

The target assembly is a tritiated titanium type target at ground potential. It is $1\frac{1}{4}$ inches in diameter

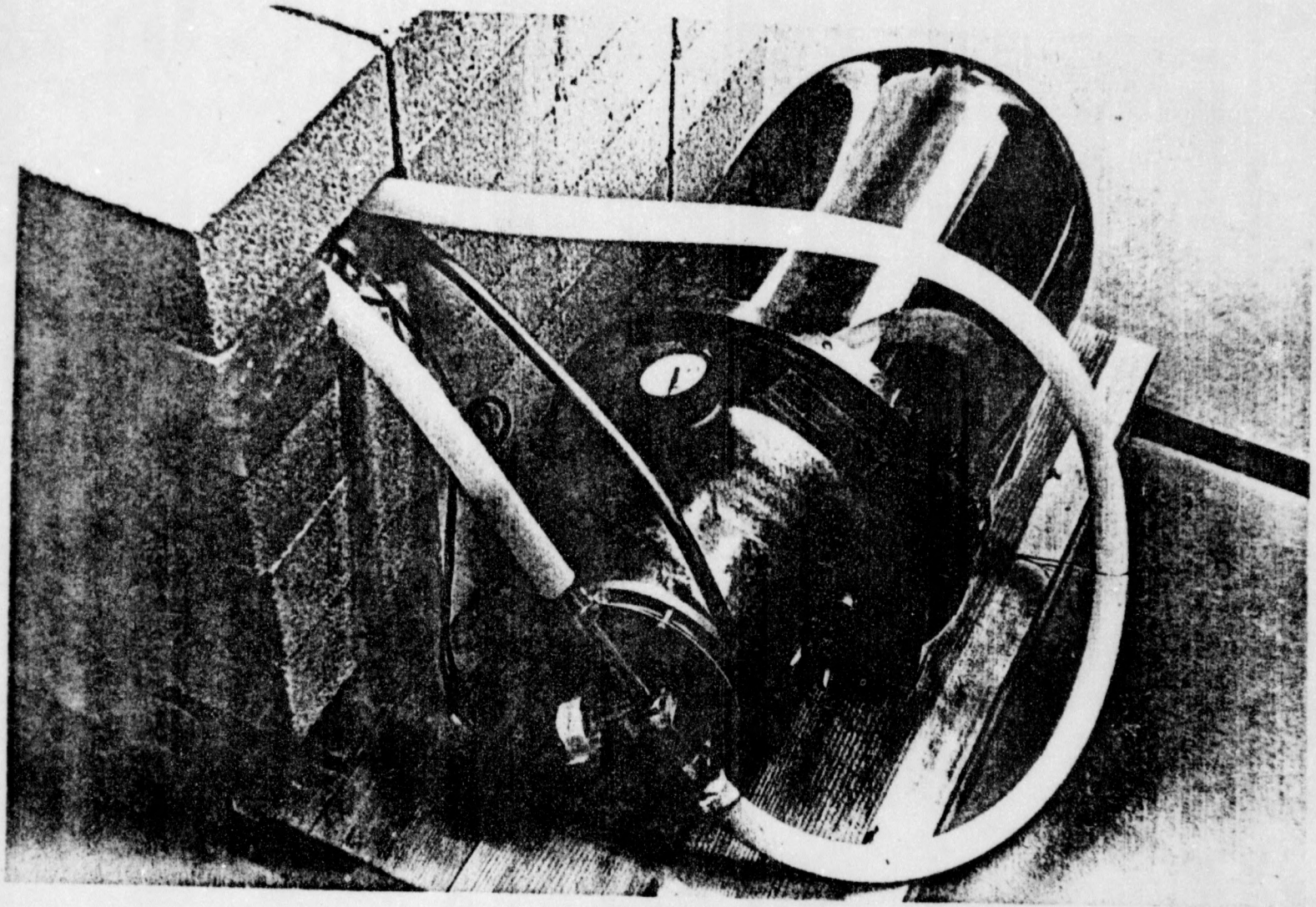

FIGURE 3. NEUTRON GENERATOR

with an active area of 6 cm^2. This target is located less than 1/8th of an inch from the external housing surface.

To provide personnel shielding during the activation of samples, the generator is located near the center of a concrete block enclosure having external dimensions of approximately 8½ feet long by 6½ feet wide by 4 feet high. To facilitate access to the generator, the shielding is constructed with a cave-like opening in one side. The generator is located on the end of a small cart behind 4 feet of concrete blocks. This cart and its contents can be rolled in and out of the opening on short tracks. This entire system is located in a ground floor room having 18 inch poured concrete walls.

Located in the cart on which the generator is situated is a slow neutron detector. This detector, a Lithium loaded plastic scintillator coupled to a photomultiplier tube, is embedded in a block of paraffin which is located 2½ feet from the neutron beam. The paraffin acts as a moderator for the fast neutrons produced by the generator. This detector is used as a monitor during the activation of the samples. The neutrons detected are used as an indication of the stability of the neutron production during activation.

The time of activation of samples and also of the elapsed time between activation and counting must be accurately known. An electronic system was built to perform these functions. The system, consisting of clocks and relays, is designed to automatically control the time of neutron

activation, the monitoring of the neutrons, the transfer of the sample on completion of activation, the measurement of elapsed time out of the neutron beam, and the starting and stopping of a multichannel analyzer. This system, including the controls for the neutron generator, the monitoring scaler, and the multichannel analyzer are shown in Figure 4.

The clocks used in the control pannel enable the time of activation, the time out of beam, and the counting time to be measured with an accuracy of 0.1%.

Counting Systems

Following activation, the radioactive samples are transferred to a counting chamber. For those samples that have well known gamma spectrums, a 3"x3" NaI(Tl) crystal is used as a detector. This crystal is coupled to an Amperex XP-1031 photomultiplier tube by means of a plexiglas light pipe. Dow Corning type 20-057 silicon grease is used to optically couple this system together. The output from the photomultiplier tube is coupled via a preamplifier to a linear amplifier. A Nuclear Data ND-180 multichannel analyzer is used to analyze the pulse height spectrum from the linear amplifier.

For those samples which decay by positron emission, the activity is determined by the coincidence method.[7] The output from two 3"x3" NaI(Tl) detectors are respectively coupled via a preamplifier and linear amplifier to timing single channel analyzers. The window width ΔE of each

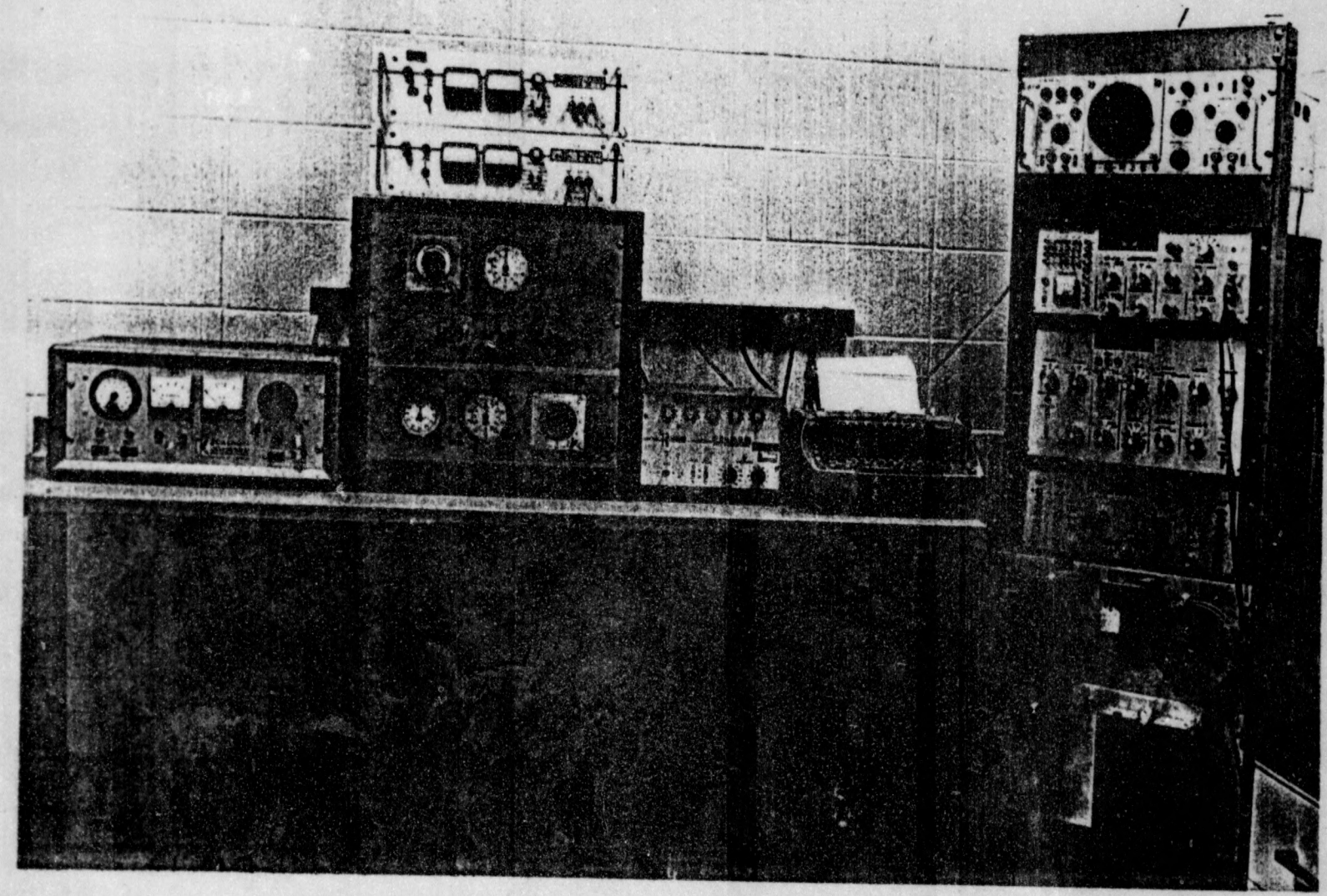

FIGURE 4. CONTROLS FOR NEUTRON GENERATOR AND MULTICHANNEL ANALYZER

timing single channel analyzer is set to accept only those pulses in the photopeak from the 0.511 MeV annihilation gamma rays. Figure 5 shows the pulse height spectrum of the annihilation gamma rays and that portion accepted by the timing single channel analyzer. The output of each timing single channel analyzer is coupled to a coincidence circuit. Three separate scalers respectively record the number of gamma rays striking each detector within ΔE along with the number of coincidence events. By counting the number of pulse heights that occur within ΔE in each timing single channel analyzer and the number of coincidence events, the activity of the sample can be calculated by the following expression:

$$A_o = \frac{N_1 N_2}{N_3} \qquad (22)$$

where A_o = absolute activity

N_1 = number of events recorded by scaler #1

N_2 = number of events recorded by scaler #2

N_3 = number of coincident events recorded by scaler #3.

If there is no correlation between events observed by each detector, this method of determination of the absolute activity of a sample is independent of the detector efficiencies. Figure 6 is a block diagram of the coincidence system. A picture of the gamma counting system and the electronics used is shown in Figure 7.

For those samples that beta decay, a NE-102 plastic scintillator 2 inches in diameter and 1½ inches long is

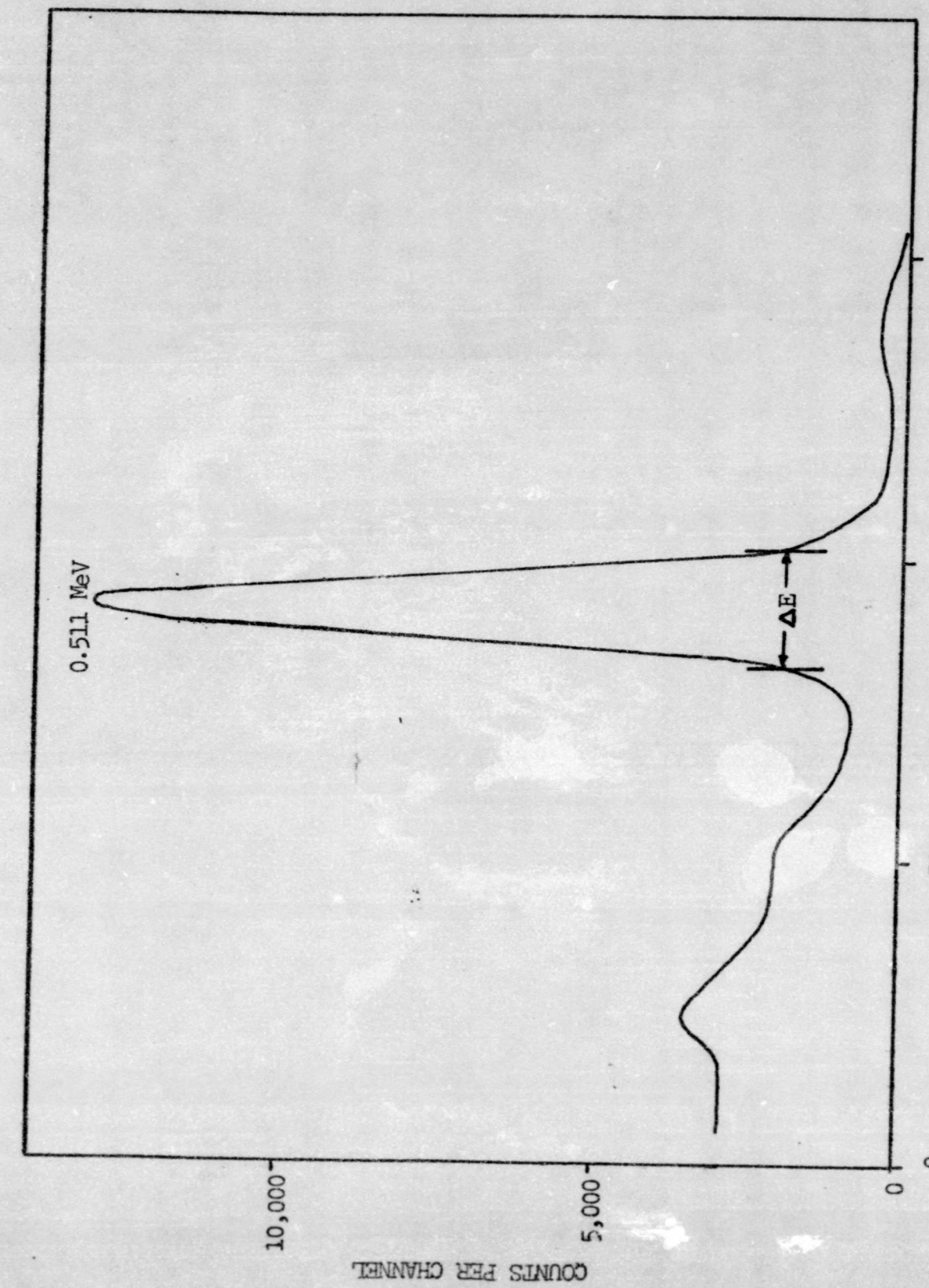

FIGURE 5. PULSE HEIGHT SPECTRUM OF ANNIHILATION GAMMA RAYS

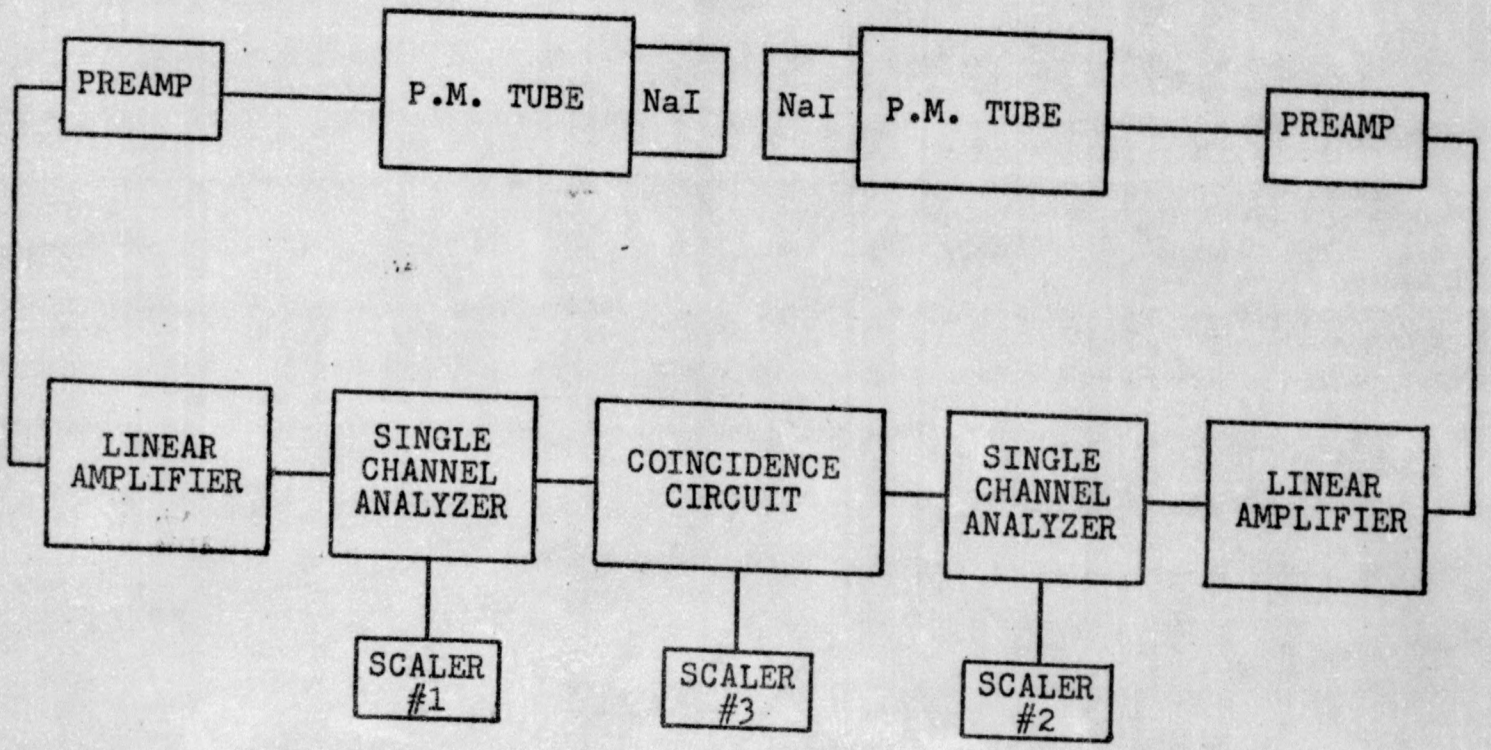

FIGURE 6. BLOCK DIAGRAM OF COINCIDENCE SYSTEM

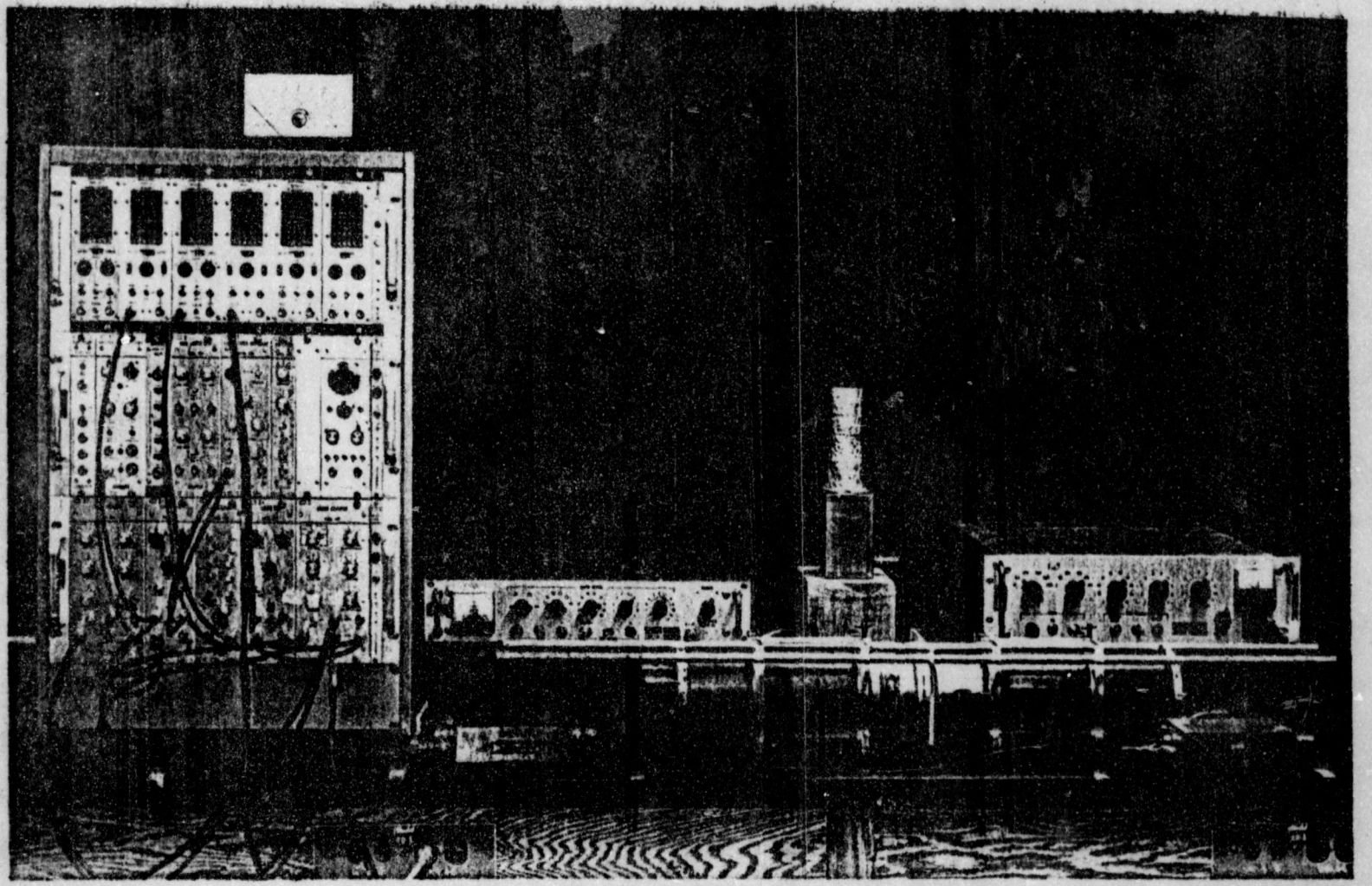

FIGURE 7. DETECTORS AND COUNTING ELECTRONICS

used as a detector. This crystal is optically coupled to an Amperex XP-1001 photomultiplier tube with Dow Corning type 20-057 silicon grease. The output of this detector is coupled via a preamplifier to a linear amplifier and then to a multichannel analyzer. The efficiency of the beta detector is determined by using a calibrated ^{32}P source. The ^{32}P source beta decays to the ground state of ^{32}S with an endpoint energy of 1.71 MeV.[8] This source satisfies two important criteria of a standard. The decay is an allowed transition[9] as is ^{70}Ga and the endpoint energy is very near that of ^{70}Ga, thus the spectra will have the same general shape.

Copper Monitors

In the determination of the (n,2n) reaction cross-sections, copper disks are used to determine the neutron flux. The choice of copper as a comparative standard is based upon the accurately measured $^{63}Cu(n,2n)^{62}Cu$ reaction cross-section of 550 $\pm$ 28 mb,[10] the high relative abundance of 69.09%, its half-life of 9.89 minutes,[8] and its decay scheme. The decay scheme for ^{62}Cu is shown in Figure 8.[8] Since ^{62}Cu decays by positron emission, the activity of the copper monitors is determined by the coincidence method previously mentioned.

The copper disks used in the determination of the (n,2n) reaction cross-sections for ^{71}Ga, ^{106}Cd, and ^{138}Ba have an average mass of 125 milligrams. These copper disks are approximately 0.4 mm thick and have the same diameter

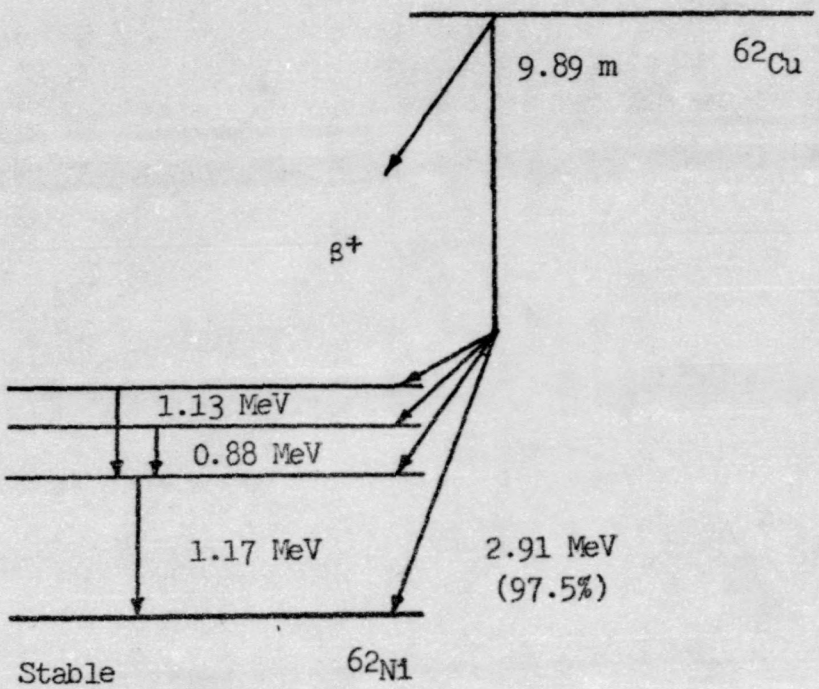

FIGURE 8. DECAY SCHEME FOR ^{62}Cu

as the sample capsules. Figure 9 shows the type of capsules used along with two copper disks.

Activation Procedure

Before activation begins, the samples to be studied are placed in small polyethylene capsules. This capsule is then carefully positioned between two copper disks which are to be used as comparative standards. Once this is done, the sample and copper disks are placed in the activation position on the face plate of the neutron generator. This positioning exposes the sample to a maximum flux of neutrons in the forward direction.

After the sample is properly positioned, the neutron beam is turned on for the preset irradiation time. At the end of irradiation, the sample and copper monitors are transferred to their respective counting chamber to be analyzed.

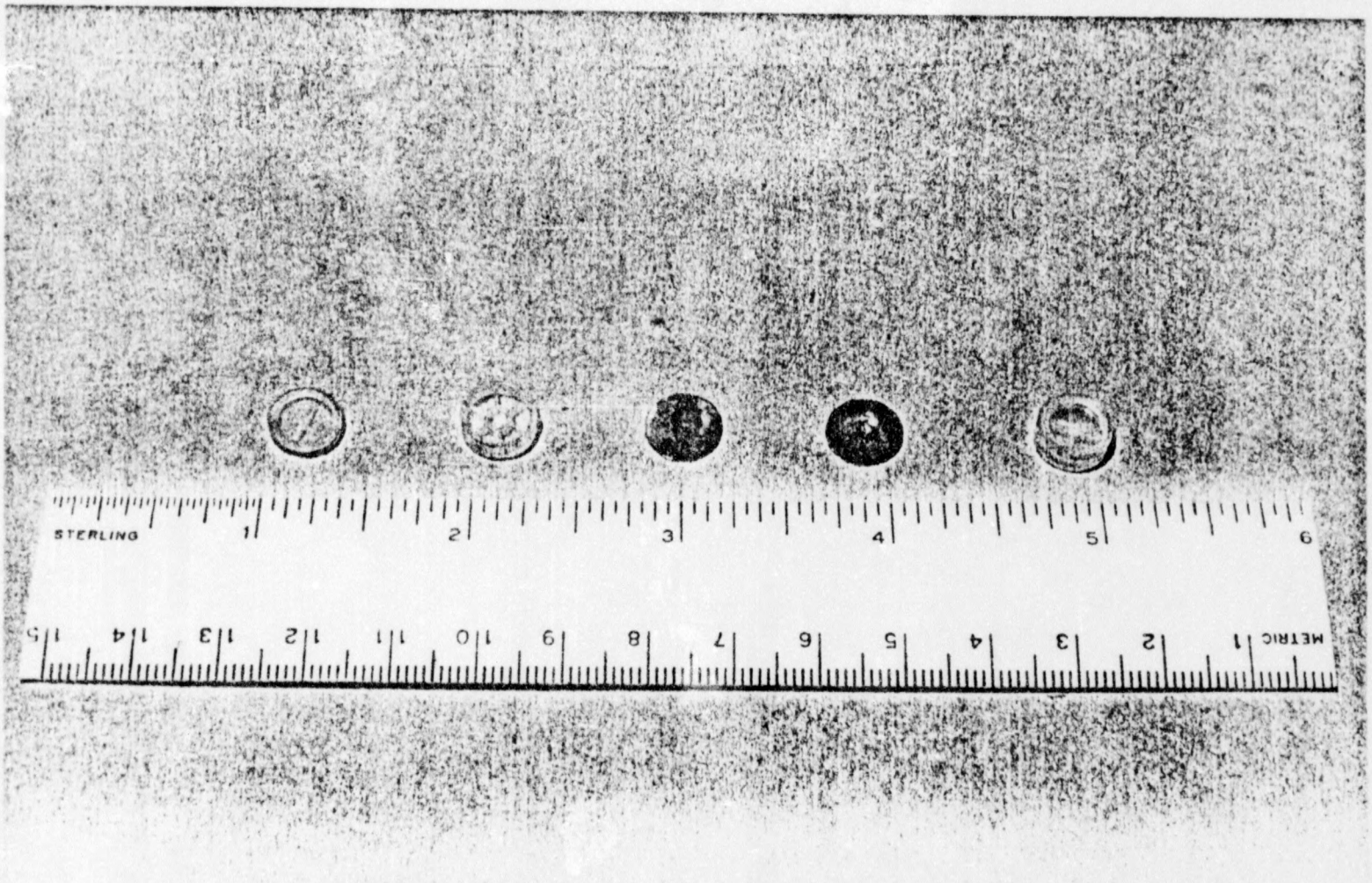

FIGURE 9. SAMPLE CONTAINERS AND COPPER DISKS

IV. EXPERIMENTAL RESULTS

$^{71}Ga(n,2n)^{70}Ga$

In a survey of the literature on (n,2n) reaction cross-sections for ^{71}Ga, two values were reported using neutrons in the 14 MeV range. Using 14.5 MeV neutrons, E. B. Paul and R. L. Clarke[1] measured the $^{71}Ga(n,2n)^{70}Ga$ reaction cross-section to be 700 mb with a standard deviation of 15%. The chemical impurity of the ^{71}Ga sample was less than 1%. During irradiation of the sample, the neutron yield was monitored by a Hanson McKibben long counter surrounded by paraffin. The average neutron flux was determined by separately irradiating thin copper disks at the activation position. The activity of the ^{70}Ga produced was measured by an end window counter.

C. S. Khurana and H. S. Hans[2] also measured the $^{71}Ga(n,2n)^{70}Ga$ reaction cross-section and obtained a value of 2180 mb with a standard deviation of 10% using 14.8 MeV neutrons. The ^{71}Ga sample used had a purity of greater than 99.9% which was determined spectroscopically. The $^{71}Ga(n,2n)^{70}Ga$ cross-section was measured by comparing it to the cross-section of the $^{56}Fe(n,p)^{56}Mn$ reaction, for which the value of 126 mb at 14.8 MeV was adopted. The activity of the irradiated sample was measured with an end-window beta counter.

The (n,2n) cross-sections are not expected to vary by factors of three over small changes in the energy of the neutrons, therefore the discrepencies in the reported values are probably the result of experimental methods. It is because of this large difference in reported cross-section values that this particular isotope was chosen.

The sample used in this part of the experiment was a 57.5 mg sample of Ga_2O_3 containing 50 mg of 99.61% enriched ^{71}Ga.[11] This sample was sealed in one of the small capsules. The sample and copper disks were then placed in the activation position and irradiated for a period of 2 minutes. Upon completion of irradiation, the sample and copper disks were transferred to their appropriate counting chambers.

The activity of the copper disks was first measured for a period of 100 seconds by the coincidence method previously mentioned. Since the ^{70}Ga produced in the $^{71}Ga(n,2n)^{70}Ga$ reaction is a beta emitter, its activity was recorded by the plactic scintillator and multichannel analyzer mentioned in Chapter III. The activity of this sample was determined by summing the number of counts in the beta spectrum recorded by the multichannel analyzer over a period of 4 minutes. This activity was then corrected for the efficiency of the detector to determine the absolute activity of the sample. Figure 10 shows the decay scheme of ^{70}Ga.[8] The beta spectrum from ^{70}Ga is shown in Figure 11.

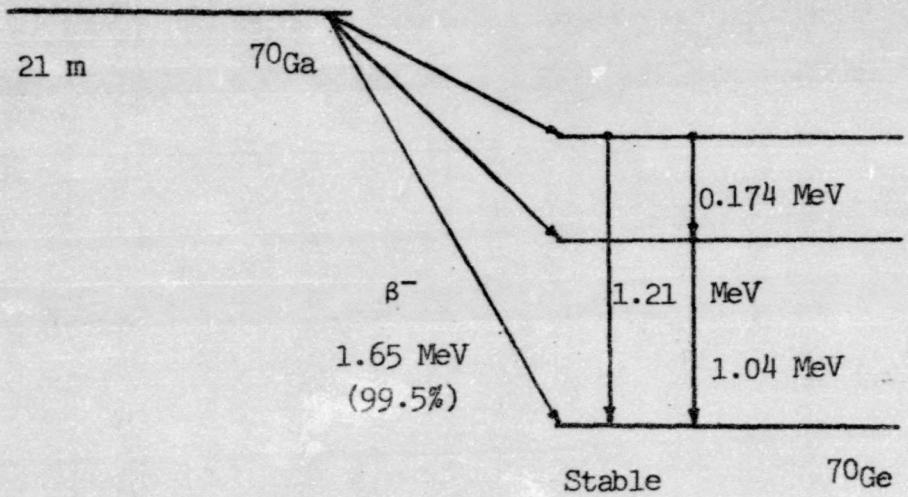

FIGURE 10. DECAY SCHEME FOR ^{70}Ga

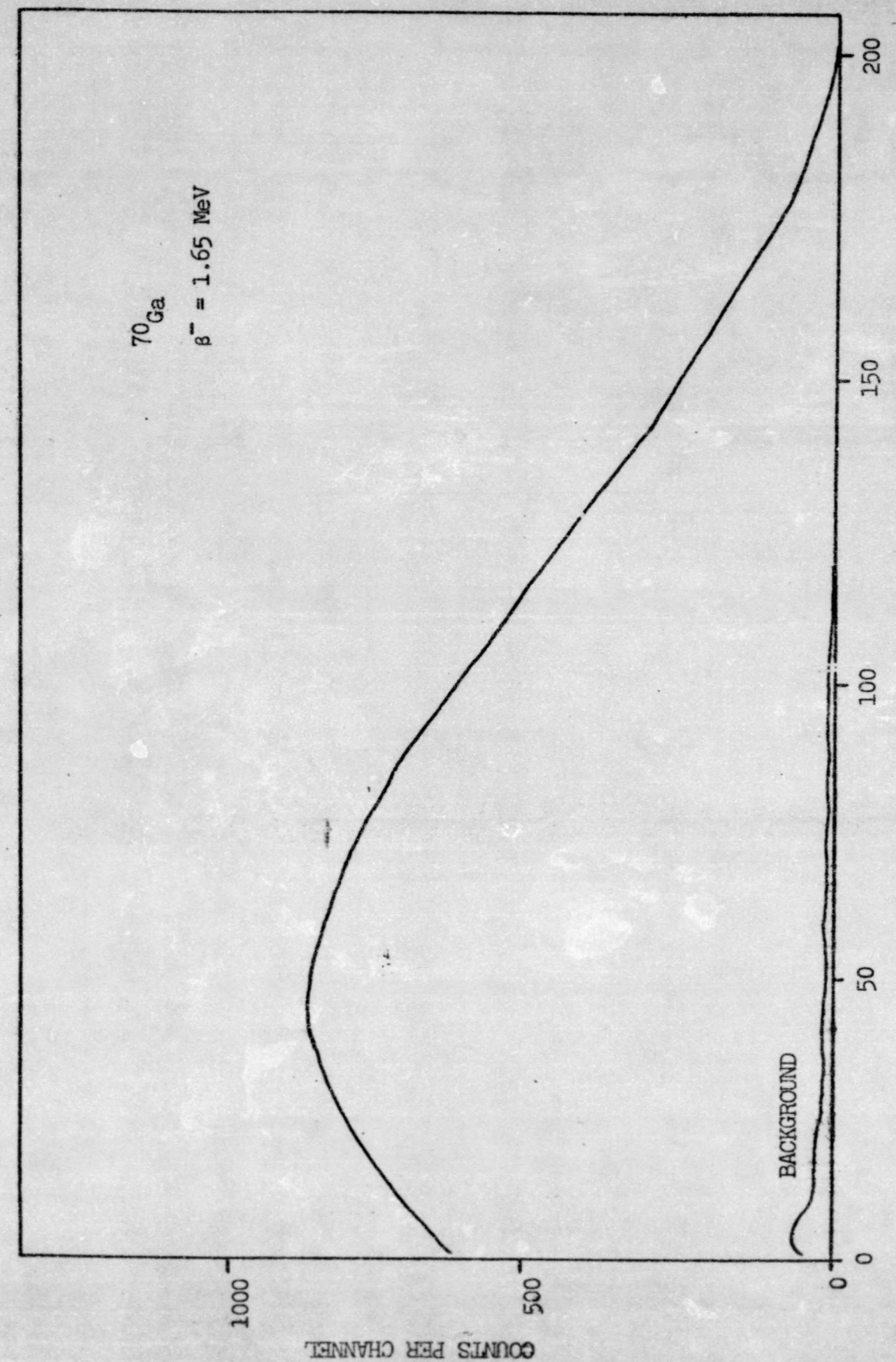

FIGURE 11. BETA PULSE HEIGHT SPECTRUM OF ^{70}Ga

Before each activation sequence was begun, the sample was monitored for a period of 4 minutes prior to activation to ensure that the activity of the previous run had been reduced to that of background radiation. In all experimental runs, background was subtracted from the observed beta spectra. Table 1 lists the values obtained for each of 10 runs and the average $^{71}Ga(n,2n)^{70}Ga$ reaction cross-section value.

$^{106}Cd(n,2n)^{105}Cd$

Two previous values for the (n,2n) reaction cross-section for ^{106}Cd have been reported by L. A. Rayburn[3] and M. Bormann et al.[4] There is a considerable difference between the values. Using neutrons of 14.4 ± .3 MeV energy Rayburn measured the reaction cross-section to be 827 ± 63 mb. Bormann, using neutrons of 12.6-19.6 MeV reported the reaction cross-section to be 1358 ± 136 mb for 14.11 MeV neutrons and 1589 ± 159 mb for 14.87 MeV neutrons. The values reported by each investigator were based upon the reaction cross-section for the $^{63}Cu(n,2n)^{62}Cu$ reaction as a comparative standard. Rayburn took this cross-section to be 503 ± 37 mb whereas Bormann used a value of 478 ± 38 mb. Each investigator determined the activity of the cadmium sample and the copper monitors by the coincidence method. The coincidence system used by Rayburn used two 1½"x1½" NaI(Tl) detectors while Bormann used two 3"x3" NaI(Tl) detectors.

TABLE 1

(n,2n) REACTION CROSS-SECTIONS FOR ^{71}Ga

Run Number	Measured Cross-section
1	1316
2	1351
3	1259
4	1224
5	1221
6	1129
7	1265
8	1237
9	1273
10	1300

$$\sigma_{av} = 1257 \pm 88 \text{ mb}$$

The large variations in the reported values for the $^{106}Cd(n,2n)^{105}Cd$ reaction cross-section indicates a need for further study. This was the basis for the selection of this particular isotope.

In this phase of the experiment, a 22.8 mg sample of CdO containing 20 mg of 88.40% enriched ^{106}Cd[11] was used. The other 11.60% of the sample was made up of the other stable cadmium isotopes. This sample along with two copper disks was irradiated for a period of 10 minutes. Upon completion of irradiation, the sample and copper disks were separated and their activities observed. The copper disks were analyzed first, by the coincidence method, for a period of 200 seconds. After this activity was recorded, the ^{105}Cd, which positron decays 55% of the time[3] was analyzed using the coincidence method for a period of 1000 seconds.

Upon completion of the counting of the ^{105}Cd activity, the sample was allowed to decay for approximately 10 hours before attempting to reactivate the sample. This decay time ensures that the activity of the sample is reduced to approximately that of background. Since the ^{105}Cd produced has a half-life of 55 minutes[8] and decays into ^{105}Ag which has a half-life of 40 days[8],(see Figure 12[8]) care had to be taken to ensure that each successive run is corrected for any activity caused by the decay of these isotopes. Before each activation sequence the cadmium sample was monitored for a period of 1000 seconds. The values obtained for each of 10 activations is listed in Table 2 along with the average $^{106}Cd(n,2n)^{105}Cd$ reaction cross-section value.

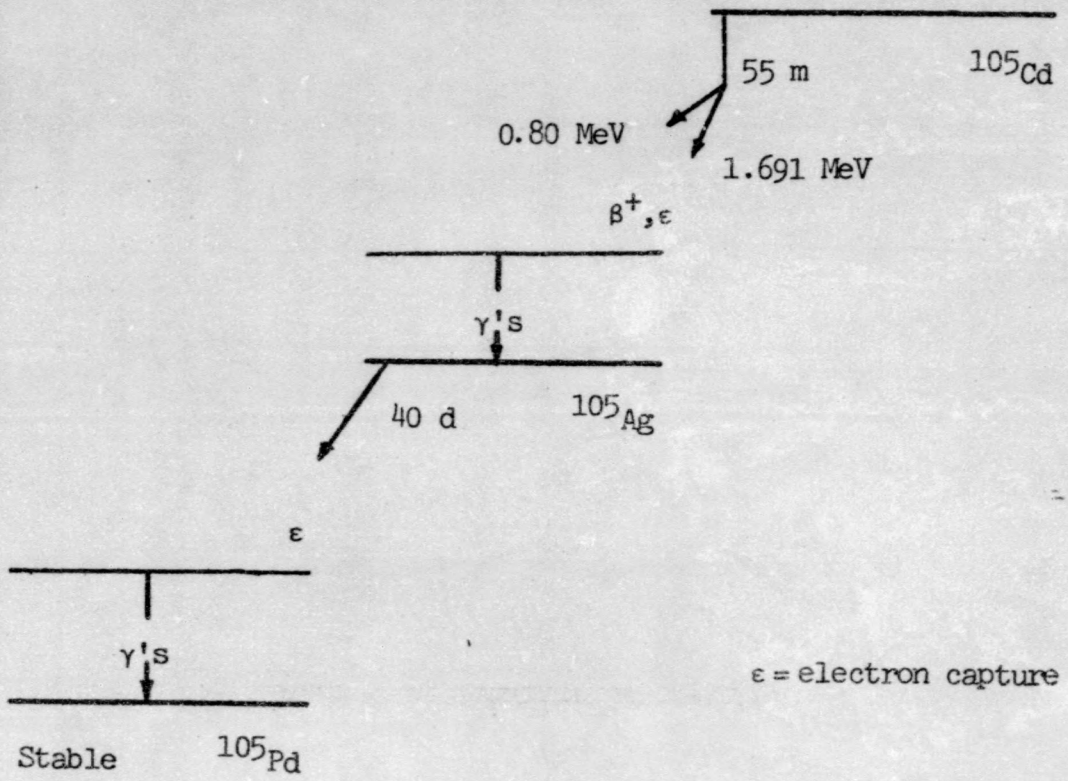

FIGURE 12. DECAY SCHEME FOR ^{105}Cd

TABLE 2

(n,2n) REACTION CROSS-SECTIONS FOR ^{106}Cd

Run Number	Measured Cross-section
1	985
2	977
3	1043
4	1009
5	1036
6	1032
7	966
8	988
9	982
10	1165

$$\sigma_{av} = 1018 \pm 71 \text{ mb}$$

$^{138}Ba(n,2n)^{137m}Ba$

A literature survey of the $^{138}Ba(n,2n)^{137m}Ba$ reaction cross-section measurements for neutrons in the 14 MeV energy range revealed only one reported value. R. G. Wille and R. W. Fink[5] determined the reaction cross-section to be 1250 $\pm$ 100 mb for neutrons of 14.8 MeV energy. This value was based upon the cross-section of 519 mb for the $^{63}Cu(n,2n)^{62}Cu$ reaction as a comparative standard. The activity of the radioactive ^{137m}Ba was measured by a methane-flow beta-proportional counter.

This sample was chosen on the basis that only one value was reported for the $^{138}Ba(n,2n)^{137m}Ba$ reaction cross-section. The barium sample used was a 152 mg sample of $Ba(NO_3)_2$ containing 80 mg of 99.80% enriched ^{138}Ba.[11] This sample along with two copper disks was irradiated for a period of 1 minute. Upon completion of irradiation, the sample and copper disks were transferred to their appropriate counting chambers.

The activity of the copper disks was determined over a period of 200 seconds by the coincidence method. The activity of the ^{137m}Ba produced in this reaction was then determined by placing the radioactive sample on the face of a 3"x3" NaI(Tl) crystal and recording the gamma spectrum on the multichannel analyzer as discussed in Chapter III. This activity was recorded for a period of 2 minutes. By summing the number of counts under the photopeak and determining the absolute efficiency and peak-to-sum ratio

from Heath,[12] the activity of the sample can be determined by equation (15) as shown in Chapter II. Figure 13 shows the decay scheme for ^{137m}Ba[8] along with that portion of the gamma ray pulse height spectrum summed.

The efficiency of the detector is a function of the source to crystal distance and was critical in this phase of the experiment. This distance was determined in two different ways. The first method used a calibrated ^{137}Cs source. This source was positioned along the axis of the crystal at various distances from the protective cover. The activity of the ^{137}Cs source was determined at each position and then adjusted to compensate for the distance between the crystal face and that of the protective covering. The second method consisted of x-raying the crystal to determine the distance from the crystal to the protective covering. Both methods indicated this distance to be 1.0 ± 0.1 cm.

Since the ^{137m}Ba half-life is 2.6 minutes,[8] a period of one hour was allowed between each activation sequence. Before each activation period, the sample was monitored for a period of 2 minutes to ensure that the activity was approximately that of the background. For all data taken of the ^{137m}Ba gamma spectra, the background radiation was subtracted. Table 3 lists the values obtained for each of 10 runs and the average $^{138}Ba(n,2n)^{137m}Ba$ reaction cross-section value.

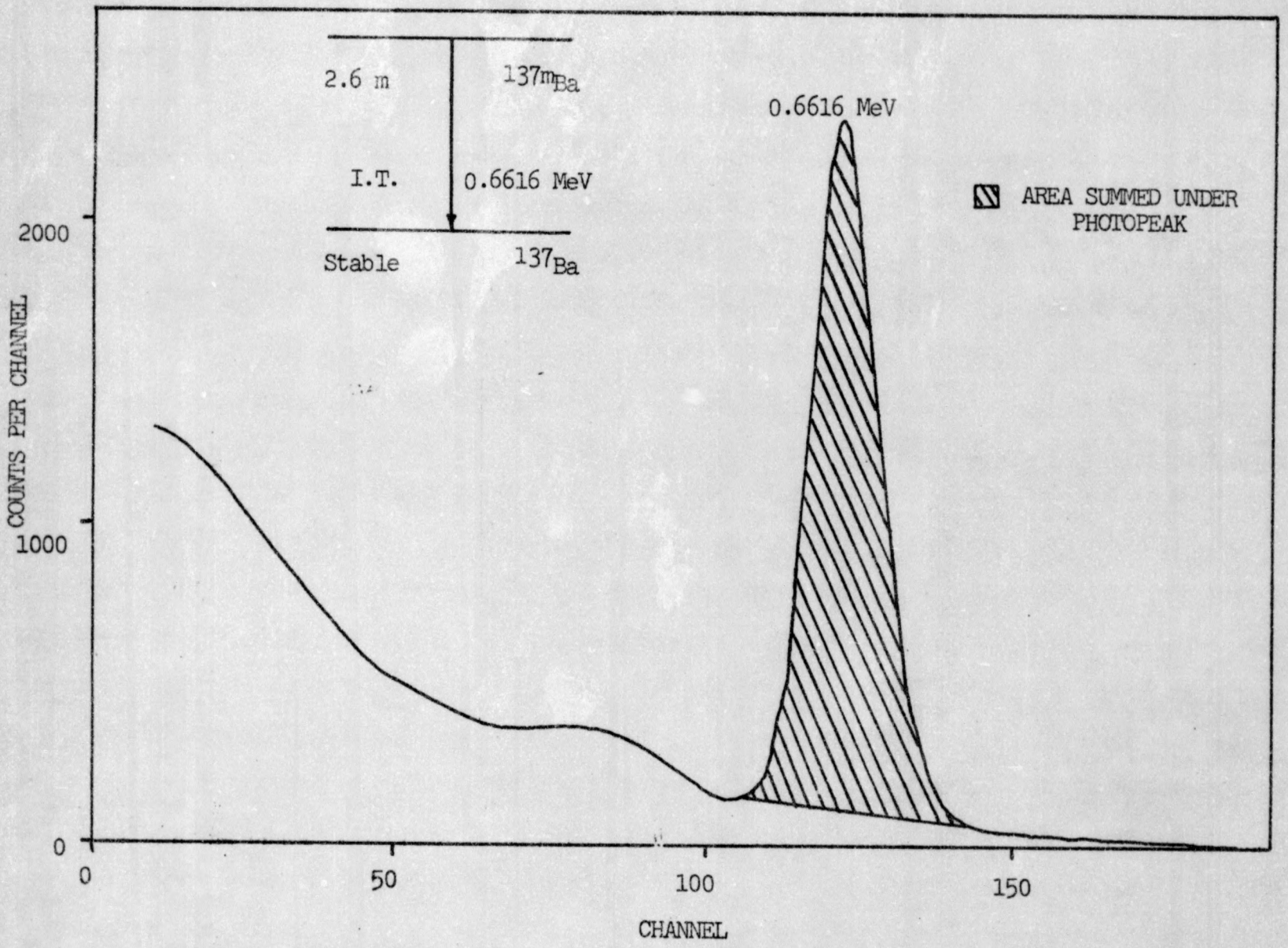

FIGURE 13. DECAY SCHEME AND GAMMA RAY PULSE HEIGHT SPECTRUM FOR ^{137m}Ba

TABLE 3

(n,2n) REACTION CROSS-SECTIONS FOR ^{138}Ba

Run Number	Measured Cross-section
1	1236
2	1307
3	1255
4	1335
5	1298
6	1299
7	1334
8	1283
9	1349
10	1293

$$\sigma_{av} = 1299 \pm 104 \text{ mb}$$

V. DISCUSSION OF RESULTS

Accomplishment of Purpose

The (n,2n) reaction cross-sections measured in this experiment are listed in Table 4 along with the previously reported values and the theoretical (n,2n) cross-sections for 14.1 MeV neutrons calculated by Pearlstein.[13] The theoretically calculated (n,2n) cross-section values are based on the statistical model and empirical expressions for inelastic cross-sections and level densities. These theoretical values serve only as an indication of the magnitude of the (n,2n) cross-section values when experimental values are not available.

The 1257 ± 88 mb value for the $^{71}Ga(n,2n)^{70}Ga$ reaction cross-section determined in this experiment lies between the 700 mb ± 15% value reported by Paul and Clarke[1] and the 2180 mb ± 10% value reported by Khurana and Hans.[2] The value obtained by Paul and Clarke is based on the activity produced in a copper sample by the $^{63}Cu(n,2n)^{62}Cu$ reaction. However, the copper standard was irradiated independent of the Ga sample, therefore differing from the method used in this experiment. The method used by Paul and Clarke assumes that the neutron flux remains constant over long periods of time and that the target produces neutrons uniformly over the entire beam cross-section. Both of these assumptions are

TABLE 4 SUMMARY OF OBSERVED AND CALCULATED CROSS-SECTIONS

REACTION	OBSERVED CROSS-SECTIONS (mb)		CALCULATED CROSS-SECTIONS (mb)
	THIS WORK	LITERATURE	
$^{71}Ga(n,2n)^{70}Ga$	1257 ± 88	700 ± 105[1] 2180 ± 218[2]	944[13]
$^{106}Cd(n,2n)^{105}Cd$	1018 ± 71	827 ± 63[3] 1358 ± 136[4]	920[13]
$^{138}Ba(n,2n)^{137m}Ba$	1299 ± 104	1250 ± 100[5]	1874[13]

poor ones at times. The method of neutron flux determination used by Khurana and Hans is similar to that used in this experiment. These investigators used the same technique of sandwiching the sample between two monitoring disks. However, the $^{56}Fe(n,p)^{56}Mn$ reaction cross-section was taken as a comparative sample for determining the $^{71}Ga(n,2n)^{70}Ga$ reaction cross-section. Comparison of the experimental value to that value reported by these investigators is difficult without access to the raw data.

The measured value of 1018 $\pm$ 71 mb for the $^{106}Cd(n,2n)^{105}Cd$ reaction cross-section also lies between the two previously reported values of 827 $\pm$ 63 mb by Rayburn[3] and 1358 $\pm$ 136 mb by Bormann et al.[4] Both investigators used the $^{63}Cu(n,2n)^{62}Cu$ reaction cross-section as a comparative means of determining the (n,2n) reaction cross-section for ^{106}Cd. The value taken for the $^{63}Cu(n,2n)^{62}Cu$ reaction cross-section by Rayburn was 503 $\pm$ 37 mb while Bormann used a value of 478 $\pm$ 38 mb. Although these values are slightly less than the 550 $\pm$ 38 mb value used in this experiment, the method used in the determination of the neutron flux differs considerably. Both investigators irradiated the samples and monitors at the same time, but the samples were placed in positions different from that of the monitors. The method of determination of the neutron flux by placing the sample between the two monitoring disks virtually ensures that both the monitoring disks and the sample are exposed to an identical neutron flux.

The 1299 ± 104 mb value measured for the $^{138}Ba(n,2n)^{137m}Ba$ reaction cross-section is in close agreement with the reported value of 1250 ± 100 mb by Wille and Fink.[5] Both the reported and measured values were based upon the $^{63}Cu(n,2n)^{62}Cu$ reaction cross-section as a comparative standard. The value taken by Wille and Fink for the (n,2n) reaction cross-section for the ^{63}Cu was 519 mb while the results of this experiment were based upon the value of 550 ± 28 mb. Using the 550 ± 28 mb value as the comparative cross-section, the results of Wille and Fink would be 1325 ± 106 mb. This value still lies within the experimental error. Wille and Fink measured the activity of the ^{137m}Ba with a methane-flow beta-proportional counter which differs from the method used in this experiment.

Experimental Errors

Errors in the measurement of the experimentally determined reaction cross-sections may be introduced by several factors:

(1) Error in neutron flux measurement. Since the cross-sections were not measured, absolutely, but by a comparative method, the error in the measurement of the neutron flux depends on the irradiation geometry and the accuracy of the cross-section of the comparative standard. The neutron energy varies with the angle of emission of the neutrons; therefore the geometry of the experiment determines to a large extent the energy spread. The error introduced by these factors was estimated to be 3%.

(2) Error introduced by the presence of thermal and scattered neutrons. Because of the small enclosure in which

the generator is housed and the large amount of hydrogenous material surrounding the target, the presence of thermal and scattered neutrons could introduce errors in the cross-section measurements for some isotopes. The possibility of thermal neutrons causing error in the determination of the reaction cross-sections can be considered negligible since the thermal neutron cross-sections for the isotopes studied are small. Even if such a reaction were to occur, the activity of the products formed would be so small that they would be considered negligible. The amount of error produced by the scattered neutrons can also be considered negligible since the scattered flux is lower by several orders of magnitude.

(3) Error in the total number of nuclei. An error in the number of nuclei present may be introduced by the presence of impurities. All samples were enriched isotopes which were analyzed spectrographically and had an extimated error of less that 1% from the known source of systematic errors. For the copper disks used as monitors, the percent of impurities was less than 0.1%. The mass of the samples and copper disks was determined to within 0.1%.

(4) Miscellaneous errors. Uncertainty in the measurement of the activation time, time out of beam and counting time would also introduce errors. These time intervals were determined to within 0.1%. The detection of gamma rays and beta particles is another source of error as was the determination of the detector efficiencies. The error due to these sources was determined to be less than 4%. The error due to the

(n,p), (n,γ) and (n,α) reactions that could occur on the isotopes studied can be considered negligible because of the small cross-section values reported for these types of reactions. The error introduced by any activity from known impurities in the samples or the presence of any oxygen and nitrogen in the form of oxides and nitrates was negligible.

Areas for Further Study

In the study of the $^{106}Cd(n,2n)^{105}Cd$ reaction cross-section, two major problems were encountered which need to be further analyzed. The decay scheme for ^{105}Cd is not well known. Several investigators[14,15] have measured the gamma transitions that occur in the decay of ^{105}Cd, but have been unable to formulate a decay scheme from their observations. The second problem is related to the first; that of the branching ratio of the number of positrons emitted to the number of electron capture processes that occur. This branching ratio was taken to be 55% in the experimental analysis of the activity of the ^{105}Cd. This branching ratio is a theoretical value calculated by Rayburn[3] using the table of allowed capture-positron ratios given by Zweifel.[16] A more accurate determination of the 14 MeV $^{106}Cd(n,2n)^{105}Cd$ reaction cross-section could be determined if this branching ratio were more accurately known.

LIST OF REFERENCES

1. Paul, E. B. and R. L. Clarke, "Cross-section Measurements of Reactions Induced by Neutrons of 14.5 MeV Energy," Canadian Journal of Physics 31, 267-277 (1953).

2. Khurana, C. S. and K. S. Hans, "Cross-Sections for (n,2n) Reactions at 14.8 MeV," Nuclear Physics 28, 560-569 (1961).

3. Rayburn, L. A., "14.4-MeV (n,2n) Cross Sections," Physical Review 122, 168-171 (1961).

4. Bormann, M., A. Behrend, I. Riehle and O. Vogel, "Investigation of (n,2n) Excitation-Functions," Nuclear Physics A115, 309-320 (1968).

5. Wille, R. G. and R. W. Fink, "Activation Cross-Sections for 14.8 MeV Neutrons and Some New Radioactive Nuclides in the Rare Earth Region," Physical Review 118, 242-248 (1960).

6. Instruction Manuel for the Model A-702 Neutron Generator, Kaman Nuclear, Colorado Springs, Colorado, 1965.

7. Chase, G. D. and J. L. Rabinowitz, Principles of Radioisotope Methodology, Burgess Publishing Co., Minneapolis, Minnesota, 1964, pp. 216-217.

8. Nuclear Data Sheets, National Academy of Science, National Research Council, Washington, D. C. (1965).

9. Wu, C. S., "The Shape of β-spectra," in Alpha-, Beta- and Gamma-Ray Spectroscopy, ed. by K. Siegbahn, North Holland Publishing Co., Amsterdam, 1965, p. 1389.

10. Glover, R. N. and E. Weigold, "Some Reaction Cross Sections for Copper and Nickel from 13.9 to 14.9 MeV Neutron Energy," Nuclear Physics 29, 309-317 (1962).

11. Isotope Sales, Oak Ridge National Laboratory, Oak Ridge, Tennessee.

12. Heath, R. L., U. S. Atomic Energy Commission Report No. IDO-16880 (1964).

13. Pearlstein, S., "An Extended Table of Calculated (n,2n) Cross Sections," Nuclear Data, Vol. 3, Section A, No. 3, 327 (1967).

14. Johnson, F. A., "The Decay of ^{105}Cd," Canadian Journal of Physics 31, 1136-1147 (1953).

15. Starke, C. L. and E. A. Phillips, "Radioactivity of ^{105}Cd and ^{106}In," Nuclear Physics A139, 33-41 (1969).

16. Zweifel, P. E., "Allowed Capture-Positron Branching Ratios," Physical Review 107, 329 (1957).